



## Letter

**Cite this article:** Jones GA, Kulessa B, Ferreira AMG, Schimmel M, Berbellini A, Morelli A (2023). Extraction and applications of Rayleigh wave ellipticity in polar regions. *Annals of Glaciology* 1–5. <https://doi.org/10.1017/aog.2023.1>

Received: 21 October 2022

Revised: 15 December 2022

Accepted: 3 January 2023

**Keywords:**

Glacier geophysics; Glacier monitoring; Sea-ice geophysics; Seismology

**Author for correspondence:**

Glenn Jones,

E-mail: [gajones@swansea.ac.uk](mailto:gajones@swansea.ac.uk)

# Extraction and applications of Rayleigh wave ellipticity in polar regions

Glenn A. Jones<sup>1,2</sup> ID, Bernd Kulessa<sup>1,3</sup> ID, Ana M. G. Ferreira<sup>2,4</sup> ID,  
Martin Schimmel<sup>5</sup> ID, Andrea Berbellini<sup>6</sup> ID and Andrea Morelli<sup>6</sup> ID

<sup>1</sup>School of Bioscience, Geography and Physics, Swansea University, Swansea, UK; <sup>2</sup>Department of Earth Sciences, University College London, London, UK; <sup>3</sup>University of Tasmania, Hobart, TAS, Australia; <sup>4</sup>CERIS, Instituto Superior Técnico, Universidade de Lisboa, Lisboa, Portugal; <sup>5</sup>Geosciences Barcelona (GEOBCN-CSIC), Barcelona, Spain and <sup>6</sup>Istituto Nazionale di Geofisica e Vulcanologia, Sezione di Bologna, Bologna, Italy

**Abstract**

Seismic Rayleigh wave ellipticity measurements are the horizontal-to-vertical ratio of the Rayleigh wave particle motion, and are sensitive to the subsurface structure beneath a seismic station. H/V ratios measured from the ambient vibrations of the Earth are being increasingly used in glaciological applications to determine glacier and ice sheet thickness, seismic velocities and firn properties. Using the newly developed degree-of-polarisation (DOP-E) method which exploits the polarisation properties of seismic noise, we identify and extract Rayleigh waves from seismic stations in Greenland, and relate them to sea ice processes and the geology of the upper crust. Finally, we provide some suggestions for future applications of DOP-E method to gain greater insight into seasonal and long-term variability of sea ice formation and breakup as well as the monitoring of ice sheet thickness, subglacial environment and firn layers in the poles.

## 1. Introduction

Rayleigh waves are seismic surface waves which travel along the Earth's surface with particle displacements with elliptical, typically retrograde motions (e.g., Aki and Richards, 2002). Ellipticity is the ratio of the horizontal-to-vertical axis of the Rayleigh wave particle motion and under ray theoretical assumptions has been shown to be dependent on the subsurface structure directly below the seismic station (e.g., Ferreira and Woodhouse, 2007). Ellipticity measurements are a powerful tool for characterising the subsurface in regions of sparse or limited seismic station coverage e.g., polar regions and are particularly responsive to the near surface structure of the Earth. The sensitivity of the ellipticity measurements are wave frequency dependent with higher frequencies having greater sensitivity to the near surface (e.g., Berbellini and others, 2019).

Rayleigh wave ellipticity from ambient noise vibrations, often also called H/V (Horizontal-to-Vertical ratio of seismic ground motion) have been used for decades by engineers and geophysicists for soil characterisation, seismic microzonation, the estimation of near surface site effects (e.g., Fäh and others, 2003; Bonnefoy-Claudet and others, 2006; Maresca and others, 2006; Poggi and others, 2012; Hobiger and others, 2013; Pastén and others, 2016) and has seen increasing application in glaciological settings to determine ice thickness, the seismic velocities of the ice and firn properties (e.g., Lévéque and others, 2010; Picotti and others, 2017; Yan and others, 2018; Köhler and others, 2019; Preiswerk and others, 2019; Yan and others, 2020; Chaput and others, 2022). Traditionally, the spectral amplitude method of Nakamura (1989) has been used to calculate H/V ratios from the Earth's ambient noise due to its stability, reliability and ease of implementation (Nakamura, 2019). However, a key assumption of the method is that the ambient noise field is dominated by Rayleigh waves which is rarely true, with the potential for H/V ratios to be strongly affected by other seismic phases such as Love waves (e.g., Bonnefoy-Claudet and others, 2008; Maranò and others, 2017; Sánchez-Sesma and others, 2019). A number of alternative methods have been developed to suppress contributions from body and Love waves on the H/V estimates (e.g., Hobiger and others, 2009; Poggi and others, 2012; Hobiger and others, 2016; Maranò and others, 2017; Berbellini and others, 2019). Berbellini and others (2019) developed an approach which uses the polarisation properties of Rayleigh waves to identify and extract them from the Earth's ambient seismic noise field. The ellipticity is subsequently computed on the extracted Rayleigh waves avoiding the issue of contamination from other seismic phases (e.g., Bonnefoy-Claudet and others, 2008; Maranò and others, 2017; Sánchez-Sesma and others, 2019).

Once estimated, the ellipticity measurements can be inverted for the 1-D vertical profiles of seismic velocities ( $V_p$  and  $V_s$ ) and density directly beneath each station. The non-linear inverse problem is solved by minimising the difference between the measured ellipticity and theoretical estimates which are usually computed using the propagator method (e.g., Aki and Richards, 2002) or normal mode approaches (e.g., Berbellini and others, 2019; Jones and others, 2021). Alternatively, approaches based on a diffuse seismic wavefield can incorporate other seismic phases into the forward modelling allowing for H/V measurements made using the spectral amplitude method of Nakamura (1989) to be inverted (e.g., García-Jerez and

© The Author(s), 2023. Published by Cambridge University Press. This is an Open Access article, distributed under the terms of the Creative Commons Attribution licence (<http://creativecommons.org/licenses/by/4.0/>), which permits unrestricted re-use, distribution and reproduction, provided the original article is properly cited.

others, 2016; Yan and others, 2018; Köhler and others, 2019; Preiswerk and others, 2019). Due to the non-linear nature of the inversion, a Monte Carlo approach is typically used to effectively sample the parameter space (e.g., Berbellini and others, 2019; Jones and others, 2021).

In this paper, we give a brief overview of the newly developed method DOP-E method of Berbellini and others (2019) which extracts Rayleigh waves from the Earth's ambient noise before computing the corresponding ellipticity. We give an overview of how these extracted Rayleigh waves can be used to track the formation and retreat of sea ice before describing the use of ellipticity to characterise the subglacial geology of Greenland. Finally, we suggest some further research directions and applications of Rayleigh waves and associated ellipticity measurements.

## 2. Degree-of-polarisation method

The method developed by Berbellini and others (2019) named DOP-E builds upon the degree-of-polarisation (DOP) method of Schimmel and Gallart (2003, 2004); Schimmel and others (2011) to identify and extract Rayleigh waves from seismic recordings. It performs a frequency-dependent moving window Eigen-decomposition on spectral matrices containing time-frequency representations of three-component seismograms (Schimmel and Gallart, 2003, 2004; Schimmel and others, 2011). This approach allows for the instantaneous semi-major and semi-minor axis of the best fitting ellipse to the data to be calculated. The vector product of the semi-major and semi-minor axes is used to define the planarity vector which should closely match the expected elliptical particle motion of the fundamental mode Rayleigh wave (Schimmel and Gallart, 2003, 2004; Schimmel and others, 2011; Sergeant and others, 2013). The DOP is then defined as the projection of the instantaneous planarity on the mean planarity vector of the frequency dependent window and varies between 0 and 1, where 0 indicates randomly changing polarisation and 1 is a stable polarisation measurement throughout the data window (Schimmel and Gallart, 2003, 2004; Schimmel and others, 2011; Sergeant and others, 2013; Berbellini and others, 2019). The method assumes that the Rayleigh wave particle motion is retrograde permitting the calculation of the back azimuth of the signal from the station to the source (Schimmel and others, 2011; Sergeant and others, 2013; Berbellini and others, 2019). Finally, the ellipticity of the extracted Rayleigh waves is estimated as a function of frequency and can subsequently be used in inversions for subsurface structure (e.g., Berbellini and others, 2019; Jones and others, 2021)

## 3. Current applications

### 3.1. Tracking sea ice formation and breakup

The Earth's ambient noise is ubiquitous and displays similar features around the globe. Specifically, the seismic noise spectra exhibit two prominent peaks corresponding to primary ( $T \sim 10-20$  s) and secondary microseisms ( $T \sim 1-10$  s) (e.g., Sergeant and others, 2013; McNamara and Boaz, 2019). These microseisms are generated through the interaction of ocean gravity waves with the ocean bottom resulting in the generation of seismic waves (e.g., Longuet-Higgins, 1950; Hasselmann, 1963; Ardhuin and others, 2019). Primary microseisms arise in shallow water from the breaking or shoaling waves and have periods equal to the generative ocean swell whilst secondary microseisms are generated through the non-linear interaction of ocean waves and can occur in both deep and shallow waters with periods equal to half that of the ocean wave (e.g., Hasselmann, 1963; Ardhuin and others, 2019; McNamara and Boaz, 2019). Typically, Rayleigh and Love waves are the dominant seismic waves observed at microseismic periods (e.g., Longuet-Higgins, 1950; Hasselmann, 1963; Ardhuin and others, 2019).

The presence of sea ice can affect the power of microseisms by inhibiting and dampening ocean waves (Stutzmann and others, 2009; Grob and others, 2011; Tsai and McNamara, 2011; Anthony and others, 2014; McNamara and Boaz, 2019). For example, Stutzmann and others (2009) correlated a reduction in both primary and secondary microseisms at the seismic station Dumont D'Urville in Antarctica with the formation of nearby sea ice. Tsai and McNamara (2011) showed similar results from Alaska where the bandwidth and power of the microseisms are reduced in winter due to the dampening of ocean waves by sea ice.

Sergeant and others (2013) and Jones and others (2021) used the DOP method to extract Rayleigh waves in the secondary microseismic frequency band from stations in Greenland and in the North Atlantic. Using the back-azimuth of the incoming Rayleigh waves the sources of these microseisms were determined. These sources showed a strong time and frequency variability where the predominant source of the microseisms are storms in the Irminger Sea and Denmark Strait in the North Atlantic (Sergeant and others, 2013) (Fig. 1) with frequencies of  $\sim 0.1-0.2$  Hz. During the summer higher frequency ( $\sim 0.2-0.3$  Hz) microseisms are seen in the direction of the Labrador Sea and Baffin Bay in response to sea ice retreat. The retreat of the sea ice allows for short period ocean waves to interact with the shallower water in the Labrador Sea and Baffin Bay resulting in higher frequency microseisms (Fig. 1). As the sea ice begins to form during the Autumn months the higher frequency microseisms in the

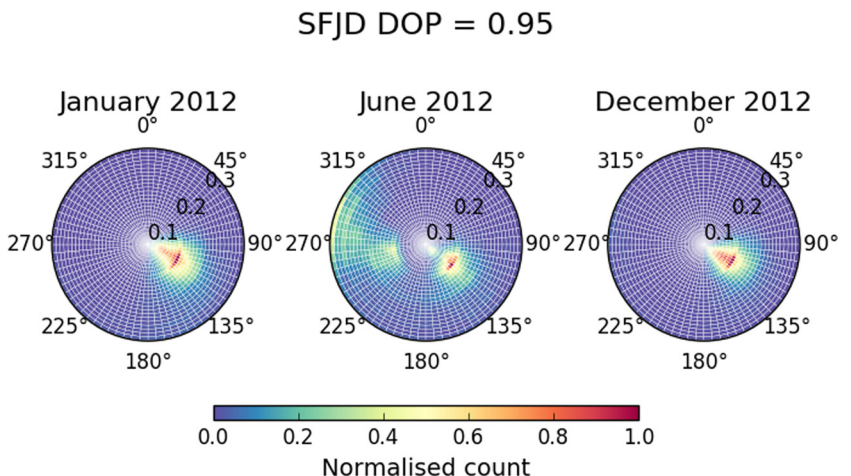


**Fig. 1.** Polar histograms of the monthly polarization direction as a function of frequency (0.1–0.3 Hz) of measured Rayleigh waves at SFJD station (Søndre Strømfjord, now Kangerlussuaq) for January, June and December 2012. Note the change in Rayleigh wave source direction and frequency content between June and the winter months (January and December).

Labrador Sea and Baffin Bay become weaker with the dominant source of Rayleigh waves returning to the Irminger Sea and the Denmark Strait in the North Atlantic.

### 3.2. Characterisation of the subglacial geology

Subglacial geology and conditions greatly control glaciers and ice sheets flow. However, the subglacial geology of Greenland is poorly understood primarily due to the presence of the ice sheet and the logistical difficulty of conducting geophysical surveys sampling the crust. Tomographic imaging using both earthquakes (e.g., Darbyshire and others, 2018; Lebedev and others, 2018; Pourpoint and others, 2018; Toyokuni and others, 2020) and ambient noise (e.g., Antonijevic and Lees, 2018; Mordret, 2018) has produced detailed images of the crust at depths >5 km due to a lack of local seismicity and large distances between seismic stations.

As explained previously, high frequency Rayleigh wave ellipticity extracted from the Earth's ambient noise is sensitive to the shallow (<5 km) structure of the Earth crust making them ideally suited to characterise subglacial geology of Greenland (e.g., Berbellini and others, 2019). Jones and others (2021) applied the DOP-E method to extract Rayleigh waves and compute their ellipticity from all available permanent seismic stations in Greenland for the period of 2012–2018 in a first attempt to characterise the seismic structure of Greenland at depth <5 km. Annual ellipticity curves were computed by calculating the mean and standard deviation of the distribution of the ellipticity measurements for each year. The ellipticity curves were then inverted using the Monte-Carlo based Neighbourhood Algorithm (Sambridge, 1999) to generate 1-D seismic shear-wave velocity ( $V_s$ ) profiles directly beneath each station.

Jones and others (2021) showed that low seismic velocities correlate with large glaciers of Jakobshavn, Helheim and Kangerdlussuaq and regions of elevated heat flux as proposed by Martos and others (2018). Jones and others (2021) inferred that the low seismic velocities within the interior of the ice sheet are the subglacial expression of the Iceland hotspot track that traversed Greenland ~80–50 Ma and controls the onset of fast ice flow for the North East Greenland Ice Stream and Petermann Glacier. This work highlights how seismic observations can provide much needed constraints on the subglacial geology and the importance of interactions between the solid Earth and overlying ice sheet.

Unique to the study of Jones and others (2021) was the use of ellipticity to characterise the subglacial geology as opposed to the ice-sheet seismic velocity or thickness as done in previous studies using H/V ratios (e.g., Lévéque and others, 2010; Picotti and others, 2017; Yan and others, 2018; Köhler and others, 2019; Preiswerk and others, 2019; Yan and others, 2020). Moreover, the study of Jones and others (2021) performed the calculation of horizontal-to-vertical amplitude ratios on extracted Rayleigh waves as a function of frequency to produce ellipticity curves as opposed to the traditional approach which calculates the spectral H/V ratio from windows of ambient noise.

### 4. Future applications

**Figure 2** compares ellipticity summary statistics (mean and standard deviation) estimated using measurements made on all available seismic data from 2015 with fundamental mode Rayleigh wave predictions obtained using a normal mode approach (Herrmann, 2013) and the model of Jones and others (2021) at the on-ice station DY2G in Greenland. There is a clear deviation between the predictions and observations at periods which are sensitive to the ice thickness ( $T < 2.5$  s). Similar deviations at ice sensitive periods were observed at Concordia station in Antarctica by Berbellini and others (2019). Berbellini and others (2019) showed that a single ice layer model was insufficient to account for this discrepancy between the predictions and observed data and that an additional near surface layer was required. Therefore, Rayleigh wave ellipticity measurements can provide insight on the internal structure of the ice in addition to the ice thickness. Additionally, ellipticity has also been shown to be sensitive to thin subglacial layers such as sediment or water which are important to understanding enhanced ice flow (Berbellini and others, 2019; Jones and others, 2021).

However, care should be taken at glaciers with ice thicknesses  $\leq 500$  m where ellipticity measurements with periods of  $\leq 2$  s are necessary to constrain the ice structure. At these short periods, the seismic noise can be highly complex containing surface wave overtones, trapped waves and reflections and also may be influenced by resonances related to the geometry of the glacier or valley (Preiswerk and others, 2019). Since the DOP-E method uses the polarisation properties of the Rayleigh waves to extract them from the Earth's ambient noise, the influence of the wave-field complexity on the measured ellipticities should be minimised, however, discriminating between the fundamental mode

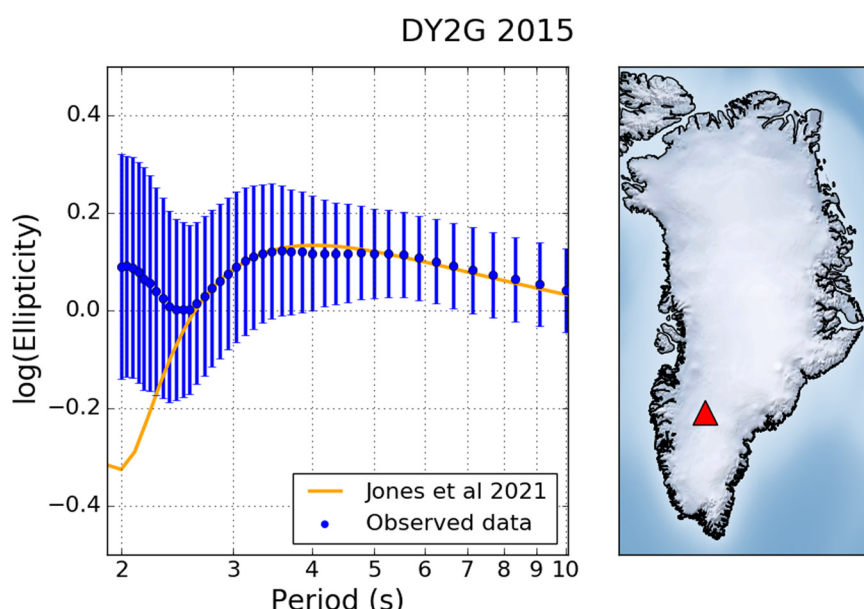


**Fig. 2.** Left: Comparison of ellipticity measurements as a function of period (blue dots and associated error bars) for on-ice station DY2G and fundamental mode fundamental mode predictions (orange line) calculated using the model of Jones and others (2021). Right: Map of Greenland with the location of DY2G (red triangle).

Rayleigh waves and overtones could prove challenging. Further analysis is needed to determine the stability of the DOP-E method for determining the ice structure of mountain glaciers.

As shown in the previous section, microseismic Rayleigh waves are sensitive to the presence of sea ice (e.g., Stutzmann and others, 2009; Grob and others, 2011; Tsai and McNamara, 2011; Anthony and others, 2014; McNamara and Boaz, 2019; Sergeant and others, 2013) and offer an approach to monitor and understand the seasonal variability in sea ice formation and breakup. In particular, it may be possible to use the DOP method to identify Rayleigh waves (or other seismic phases) with characteristic signatures and events such as changes in amplitude and back-azimuths associated with the cracking of sea ice (Kaminuma, 1994). Glacier and ice sheets near-surface and sub-glacial environments also undergo dramatic seasonal variations which should also have a significant effect on the ellipticity measurements at periods sensitive to ice. Seasonal variations in ellipticity could then be used to characterise and monitor changes in the near-surface firn. In addition, a number of seismic stations deployed in polar regions have long deployment histories (e.g., Concordia station in Antarctica which was installed in 1982) and can offer annual and decadal insights into the variability of sea ice and the state of the glacier. Finally, the installation of passive seismic instruments in polar regions is relatively quick and cheap when compared to lengthy active geophysical field campaigns and offers a convenient method of continuous in-situ monitoring of glaciers, ice sheets and sea ice.

**Acknowledgements.** G.A.J. is funded through the by the Sêr Cymru II Program in Low Carbon Energy and the Environment (European Regional Development Fund and Welsh European Funding Office; Project number 80761-SU-SU093). A.M.G.F. is grateful to support from NERC grant NE/N011791/1. M.S. thanks SANIMS (RTI2018-095594-B-I00). This project has received funding from the European Research Council (ERC) under the European Union's Horizon 2020 research and innovation program (grant agreement No 101001601). The authors would like to thank an anonymous reviewer and Douglas MacAyeal for their constructive comments and suggestions for the manuscript.

## References

- Aki K and Richards PG (2002) *Quantitative Seismology*. Melville, NY, USA: University Science Books.
- Anthony RE and 8 others (2014) The seismic noise environment of Antarctica. *Seismological Research Letters* **86**(1), 89–100.
- Antonijevic SK and Lees JM (2018) Effects of the Iceland plume on Greenland's lithosphere: new insights from ambient noise tomography. *Polar Science* **17**, 75–82.
- Ardhuin F, Gualtieri L and Stutzmann E (2019) Physics of ambient noise generation by ocean waves. In Nakata N Gualtieri L and Fichtner A (eds), *Seismic Ambient Noise*. Cambridge, UK: Cambridge University Press, pp. 69–108.
- Berbellini A, Schimmel M, Ferreira AM and Morelli A (2019) Constraining S-wave velocity using Rayleigh wave ellipticity from polarization analysis of seismic noise. *Geophysical Journal International* **216**(3), 1817–1830.
- Bonnefoy-Claudet S and 6 others (2006) H/V ratio: a tool for site effects evaluation. results from 1-D noise simulations. *Geophysical Journal International* **167**(2), 827–837.
- Bonnefoy-Claudet S, Köhler A, Cornou C, Wathelet M and Bard PY (2008) Effects of love waves on microtremor H/V ratio. *Bulletin of the Seismological Society of America* **98**(1), 288–300.
- Chaput J, Aster R, Karplus M and Nakata N (2022) Ambient high-frequency seismic surface waves in the firn column of central west Antarctica. *Journal of Glaciology* **68**(270), 785–798.
- Darbyshire FA, Dahl-Jensen T, Larsen TB, Voss PH and Joyal G (2018) Crust and uppermost-mantle structure of Greenland and the Northwest Atlantic from Rayleigh wave group velocity tomography. *Geophysical Journal International* **212**(3), 1546–1569.
- Fäh D, Kind F and Giardini D (2003) Inversion of local S-wave velocity structures from average H/V ratios, and their use for the estimation of site-effects. *Journal of Seismology* **7**(4), 449–467.
- Ferreira AM and Woodhouse JH (2007) Source, path and receiver effects on seismic surface waves. *Geophysical Journal International* **168**(1), 109–132.
- García-Jerez A, Piña-Flores J, Sánchez-Sesma FJ, Luzón F and Perton M (2016) A computer code for forward calculation and inversion of the H/V spectral ratio under the diffuse field assumption. *Computers & Geosciences* **97**, 67–78.
- Grob M, Maggi A and Stutzmann E (2011) Observations of the seasonality of the Antarctic microseismic signal, and its association to sea ice variability. *Geophysical Research Letters* **38**(11), L11302.
- Hasselmann K (1963) A statistical analysis of the generation of microseisms. *Reviews of Geophysics* **1**(2), 177–210.
- Herrmann RB (2013) Computer programs in seismology: an evolving tool for instruction and research. *Seismological Research Letters* **84**(6), 1081–1088.
- Hobiger M and 9 others (2013) Ground structure imaging by inversions of Rayleigh wave ellipticity: sensitivity analysis and application to European strong-motion sites. *Geophysical Journal International* **192**(1), 207–229.
- Hobiger M, Bard PY, Cornou C and Le Bihan N (2009) Single station determination of Rayleigh wave ellipticity by using the random decrement technique (RayDec). *Geophysical Research Letters* **36**(14), L14303.
- Hobiger M, Cornou C, Bard PY, Le Bihan N and Imperatori W (2016) Analysis of seismic waves crossing the Santa Clara Valley using the three-component MUSICUE array algorithm. *Geophysical Journal International* **207**(1), 439–456.
- Jones GA and 5 others (2021) Uppermost crustal structure regulates the flow of the Greenland ice sheet. *Nature Communications* **12**(1), 1–12.
- Kaminuma K (1994) Seismic activity in and around the Antarctic continent. *Terra Antarctica* **1**, 423–426.
- Köhler A, Maupin V, Nuth C and van Pelt W (2019) Characterization of seasonal glacial seismicity from a single-station on-ice record at Holtedahlfonna, Svalbard. *Annals of Glaciology* **60**(79), 23–36.
- Lebedev S, Schaeffer AJ, Fullea J and Pease V (2018) Seismic tomography of the Arctic region: inferences for the thermal structure and evolution of the lithosphere. *Geological Society, London, Special Publications* **460**(1), 419–440.
- Lévéque JJ, Maggi A and Souriau A (2010) Seismological constraints on ice properties at dome C, Antarctica, from horizontal to vertical spectral ratios. *Antarctic Science* **22**(5), 572–579.
- Longuet-Higgins MS (1950) A theory of the origin of microseisms. *Philosophical Transactions of the Royal Society of London. Series A, Mathematical and Physical Sciences* **243**(857), 1–35.
- Maranò S, Hobiger M and Fäh D (2017) Retrieval of Rayleigh wave ellipticity from ambient vibration recordings. *Geophysical Journal International* **209**(1), 334–352.
- Maresca R, Galluzzo D and Del Pezzo E (2006) H/V spectral ratios and array techniques applied to ambient noise recorded in the Colfiorito Basin, Central Italy. *Bulletin of the Seismological Society of America* **96**(2), 490–505.
- Martos YM and 5 others (2018) Geothermal heat flux reveals the Iceland hot-spot track underneath Greenland. *Geophysical Research Letters* **45**(16), 8214–8222.
- McNamara DE and Boaz RI (2019) Visualization of the seismic ambient noise spectrum. In Nakata N Gualtieri L and Fichtner A (eds), *Seismic Ambient Noise*. Cambridge, UK: Cambridge University Press, pp. 1–29.
- Mordret A (2018) Uncovering the Iceland hot spot track beneath Greenland. *Journal of Geophysical Research: Solid Earth* **123**(6), 4922–4941.
- Nakamura Y (1989) A method for dynamic characteristics estimation of subsurface using microtremor on the ground surface. *Railway Technical Research Institute, Quarterly Reports* **30**(1).
- Nakamura Y (2019) What is the Nakamura method? *Seismological Research Letters* **90**(4), 1437–1443.
- Pastén C and 5 others (2016) Deep characterization of the Santiago Basin using HVSR and cross-correlation of ambient seismic noise. *Engineering Geology* **201**, 57–66.
- Picotti S, Francese R, Giorgi M, Pettenati F and Carcione JM (2017) Estimation of glacier thicknesses and basal properties using the horizontal-to-vertical component spectral ratio (HVSR) technique from passive seismic data. *Journal of Glaciology* **63**(238), 229–248.
- Poggi V, Fäh D, Burjanek J and Giardini D (2012) The use of Rayleigh-wave ellipticity for site-specific hazard assessment and microzonation: application to the city of Lucerne, Switzerland. *Geophysical Journal International* **188**(3), 1154–1172.

- Pourpoint M, Anandakrishnan S and Ammon CJ** (2018) High-Resolution Rayleigh wave group velocity variation beneath Greenland. *Journal of Geophysical Research: Solid Earth* **123**(2), 1516–1539.
- Preiswerk LE, Michel C, Walter F and Fäh D** (2019) Effects of geometry on the seismic wavefield of Alpine glaciers. *Annals of Glaciology* **60**(79), 112–124.
- Sambridge M** (1999) Geophysical inversion with a neighbourhood algorithm—I. searching a parameter space. *Geophysical Journal International* **138**(2), 479–494.
- Sánchez-Sesma FJ and 9 others** (2011) A theory for microtremor H/V spectral ratio: application for a layered medium. *Geophysical Journal International* **186**(1), 221–225.
- Schimmel M and Gallart J** (2003) The use of instantaneous polarization attributes for seismic signal detection and image enhancement. *Geophysical Journal International* **155**(2), 653–668.
- Schimmel M and Gallart J** (2004) Degree of polarization filter for frequency-dependent signal enhancement through noise suppression. *Bulletin of the Seismological Society of America* **94**(3), 1016–1035.
- Schimmel M, Stutzmann E, Arduuin F and Gallart J** (2011) Polarized Earth's ambient microseismic noise. *Geochemistry, Geophysics, Geosystems* **12**(7), Q07014.
- Sergeant A and 5 others** (2013) Frequency-dependent noise sources in the North Atlantic Ocean. *Geochemistry, Geophysics, Geosystems* **14**(12), 5341–5353.
- Stutzmann E, Schimmel M, Patau G and Maggi A** (2009) Global climate imprint on seismic noise. *Geochemistry, Geophysics, Geosystems* **10**(11).
- Toyokuni G, Matsuno T and Zhao D** (2020) P wave tomography beneath Greenland and surrounding regions: I. crust and upper mantle. *Journal of Geophysical Research: Solid Earth* **125**(12), e2020JB019837.
- Tsai VC and McNamara DE** (2011) Quantifying the influence of sea ice on ocean microseism using observations from the Bering Sea, Alaska. *Geophysical Research Letters* **38**(22), L22502.
- Yan P and 5 others** (2018) Antarctic ice sheet thickness estimation using the horizontal-to-vertical spectral ratio method with single-station seismic ambient noise. *The Cryosphere* **12**(2), 795–810.
- Yan P, Li Z, Li F, Yang Y and Hao W** (2020) Antarctic ice-sheet structures retrieved from P-wave coda autocorrelation method and comparisons with two other single-station passive seismic methods. *Journal of Glaciology* **66**(255), 153–165.